LUND UNIVERSITY

Direction of Arrival Estimation with Arbitrary Virtual Antenna Arrays using Low Cost Inertial Measurement Units

Yaqoob, Muhammad Atif; Tufvesson, Fredrik; Mannesson, Anders; Bernhardsson, Bo

Link to publication

Direction of Arrival Estimation with Arbitrary Virtual Antenna Arrays using Low Cost Inertial Measurement Units

Muhammad Atif Yaqoob*, Fredrik Tufvesson*, Anders Mannesson†, Bo Bernhardsson†

*Dept. of Electrical and Information Technology, Lund University, Lund, Sweden

†Dept. of Automatic Control, Lund University, Lund, Sweden

Email: atif.yaqoob@eit.lth.se

Abstract—**In this paper, we have investigated the use of virtual antenna arrays at the receiver to do single antenna direction-of-arrival estimation. The array coordinates are obtained by doing simple dead reckoning using acceleration and angular speed measurements from a low cost micro-electro-mechanical system inertial measurement unit (IMU). The proposed solution requires no extra hardware in terms of receiver chains and antenna elements. Direction-of-arrival estimation results are obtained using a high resolution SAGE algorithm. Measurement results show that the direction-of-arrival can be estimated with a reasonable accuracy in an indoor environment.**

Index Terms—**Virtual Antenna Array, Direction of Arrival, Inertial Measurement Unit**

I. INTRODUCTION

In radio communications, direction-of-arrival (DoA) estimation of the radio wave has been an interesting area of research as it offers several interesting benefits in terms of improved Quality-of-Service, such as, better coverage, more reliable communication, and higher data rates [1]. Furthermore, by triangulation, the DoA information can also be used for positioning or localization in a wireless cellular network.

One of the biggest challenges to get the direction-of-arrival at a mobile handheld terminal is the extra hardware, e.g., the additional antenna elements and/or receive chains that are required to form real antenna arrays or switched arrays. Due to these practical issues, as it will increase the size and weight of the device, it has not been considered to be a feasible solution to form a larger antenna array at the mobile terminal side. To solve these issues, a virtual antenna array technique can be used by moving the receiver antenna to various locations and then measuring the radio signal at those locations, one by one, assuming that the radio channel remains constant during the measurement time. In the literature, an effort is made to employ virtual antenna arrays for DoA estimation using single antenna devices as presented in [2], [3].

In [2], a virtual array was formed using a rotating arm controlled by a motor. The rotating arm provide a uniform circular array which was used to perform high resolution DoA estimation of the radio channel. Similarly, in [3], with the help of a personal computer and a motor, the authors have used a controlled movement of the antenna where the antenna was also coupled with an inertial measurement unit (IMU). From the IMU measurements of rotational speed and lateral acceleration, the radius of the circle was estimated to form a virtual uniform circular array for further processing.

In this paper, we demonstrate DoA estimation using virtual antenna arrays where the array coordinates are estimated from raw IMU measurements for arbitrary free movements carried out in 3D. The contribution of this work is that we have demonstrated a method to perform DoA estimation with single antenna devices using virtual arrays and random movements. Indoor measurements are performed to measure the radio signal synchronously with the IMU data while moving the Rx antenna, attached with an IMU, in 3D. The results obtained from these measurements are very promising and allows for further research work in the DoA based localization in wireless cellular networks, where single antenna devices are used at the receiver.

The rest of the paper is organized as follows. A brief overview of virtual antenna arrays is provided in section II, which is followed by the description of array coordinate estimation using IMU measurements in section III. Then, the DoA estimation algorithm (SAGE) is introduced in section IV where it is also used to compute DoA estimates. The measurement setup is explained in section V, and measurement results are provided in section VI. Finally, the paper is concluded in section VII.
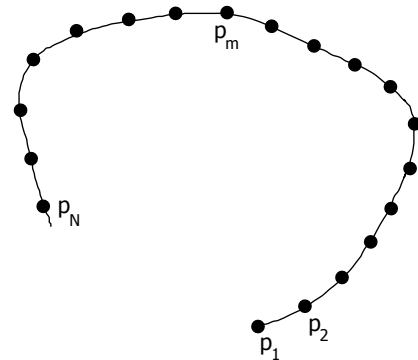

Fig. 1. Virtual antenna array for N receive antenna positions.

II. VIRTUAL ANTENNA ARRAY

The virtual antenna array is based on one Rx antenna to receive the incoming radio signal and one Rx chain for down conversion and signal processing. Array coordinates corresponding to the different antenna locations are used in the DoA estimation algorithm where the phase and amplitude differences among antenna elements are used to estimate the DoA of the incoming radio wave in the azimuth (ϕ) as well as in elevation (θ). Fig. 1 shows a virtual array where the radio signal is received at N different locations. The radio signal received at antenna position p_m has the following signal model [1],

$$r_{p_m}(t) = s(t) * h_{p_m}(t, \tau, \phi, \theta) + n_{p_m}(t), \qquad (1)$$

where $*$ denotes convolution, and $s(t)$ is the transmitted signal and is assumed to be known. Without loss of generality, we assume $s(t) = 1$, and $n_{p_m}(t)$ is assumed to be additive white Gaussian noise measured at the mth antenna position. The channel impulse response $h_{p_m}(t, \tau, \phi, \theta)$, assuming that the received signal is a sum of finite number of plane waves, is given by

$$h_{p_m}(t, \tau, \phi, \theta) = \sum_i \alpha_i(t)\delta(t - \tau_i)\delta(\phi - \phi_i)\delta(\theta - \theta_i), \quad (2)$$

where α_i, τ_i, ϕ_i and θ_i are the complex signal amplitude, delay, DoA in azimuth, and DoA in elevation of the ith multi-path component (MPC), respectively.

Fig. 2 shows how the incoming radio signal at different Rx antenna locations in a 3D space can be projected onto the different coordinate axes. The steering vector of the virtual array formed by the measurements at positions p_m can thus thus be expressed as

$$\mathbf{a}(\phi, \theta) = \exp(-jk(\mathbf{x}\sin(\theta)\cos(\phi) + \\ \mathbf{y}\sin(\theta)\sin(\phi) + \mathbf{z}\cos(\theta))), \qquad (3)$$
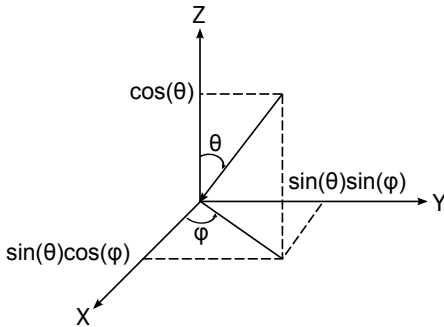

Fig. 2. Received radio signal direction vector projected on X-, Y- ,and Z-axis.

where $\mathbf{x}, \mathbf{y}$, and $\mathbf{z}$ are the position coordinate vectors of the antenna array for x-, y-, and z-axis respectively.

III. ARRAY COORDINATES

For conventional virtual antenna arrays, array coordinates are precisely controlled through controlled robotic movements and these coordinates are used for virtual array processing in DoA estimation. However, by attaching an IMU with the Rx antenna, the array coordinates for any arbitrary movement can be estimated from the IMU measurements. The IMU measurements provide raw acceleration and rotational speed in the three axes, i.e., the x-, y-, and z-axis. Local array coordinates are then obtained by computing an attitude estimate followed by a position estimate of the IMU.

A. Attitude Estimation

When the device is static, the only force acting upon the device is gravity. The acceleration due to gravity has to be subtracted to compute the net acceleration that is experienced by the device for any movement. Also, the measured acceleration from the device is in body coordinate system ($\mathbf{b}$), which is changing with the device movement. Position displacement of the device has to be determined in the earth coordinate system ($\mathbf{e}$), which is fixed.

The device orientation determines the projection of gravity acceleration onto the different axes in a coordinate system. Firstly, when the device is static, the initial orientation of the device is determined. The device orientation is represented in the form of a unit quaternion [7] which is initialized as follows

$$\mathbf{q} = \begin{bmatrix} q_0 \\ q_1 \\ q_2 \\ q_3 \end{bmatrix} = \begin{bmatrix} \cos(\vartheta/2) \\ \mathbf{u} \cdot \sin(\vartheta/2) \end{bmatrix}, \qquad (4)$$

where $\mathbf{q}$ is the unit quaternion, ϑ is the rotation angle between the earth coordinate system and the body coordinate system, and $\mathbf{u}$ is an orthonormal axis vector which is orthogonal to the two coordinate systems. The axis vector $\mathbf{u}$ is given by,

$$\mathbf{u} = \frac{\mathbf{b} \times \mathbf{e}}{|\mathbf{b}| \cdot |\mathbf{e}| \cdot \sin\vartheta}. \qquad (5)$$

Fig. 3 shows how the measurements in body coordinate system are converted to earth coordinate system through a rotation matrix defined as R^{eb} as given in (6).

Furthermore, during any movement, the measured rotational speed from the gyroscope measurements provide the orientation update information for the IMU. The quaternions are updated using (7) which assumes that the rotation speed is constant during the sample time T_s

$$R^{eb}(\mathbf{q}) = \begin{bmatrix} q_0^2 + q_1^2 - q_2^2 - q_3^2 & 2q_1q_2 + 2q_0q_3 & 2q_1q_3 - 2q_0q_2 \\ 2q_1q_2 - 2q_0q_3 & q_0^2 - q_1^2 + q_2^2 - q_3^2 & 2q_2q_3 + 2q_0q_1 \\ 2q_1q_3 + 2q_0q_2 & 2q_2q_3 - 2q_0q_1 & q_0^2 - q_1^2 + q_2^2 + q_3^2 \end{bmatrix} \qquad (6)$$

$$\mathbf{q}_n = \mathbf{q}_{n-1} + \frac{T_s}{2} S(\mathbf{q}_{n-1}) \mathbf{w}_n, \qquad (7)$$

where $\mathbf{w}$ is the 3-axis gyro measurement and $S(\mathbf{q})$ is defined as,

$$S(\mathbf{q}) = \begin{bmatrix} -q_1 & -q_2 & -q_3 \\ q_0 & -q_3 & q_2 \\ q_3 & q_0 & -q_1 \\ -q_2 & q_1 & q_0 \end{bmatrix}. \qquad (8)$$

B. Position Estimation

Once the device acceleration in the earth coordinate system is determined, then by doing double integration of the acceleration values, we can estimate the position displacement in the x-, y-, and z-axes respectively. Fig. 4 shows a block diagram for determining the array coordinates from the IMU measurements.

In Fig. 4, $\mathbf{w}^b$ is the rotational speed and $\mathbf{a}^b$ is linear acceleration measurement from the IMU, $\mathbf{g}^e$ is the acceleration due to gravity defined in the earth coordinate system, and $\mathbf{p}^e$ contains the x-, y-, and z-axis position estimates in the earth coordinate system. The figure shows that gravity acceleration is subtracted from the IMU measurements to compute net acceleration due to movement which further provides the position estimates.

IV. DoA Estimation

Using the local array coordinates and the received wideband radio signal at these locations, high resolution parameter estimation of the multi-path components (MPCs) can be performed using, e.g., SAGE [4]. By using an iterative method,
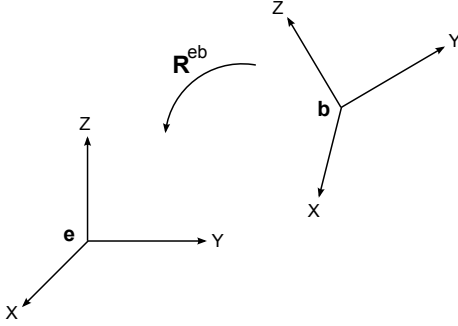

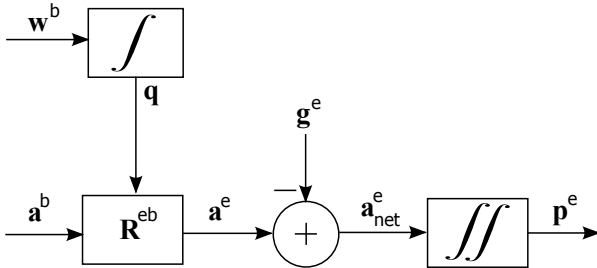Fig. 3. Body coordinate system to earth coordinate system.

Fig. 4. Position estimation from the IMU measurements.

the SAGE algorithm provide maximum likelihood estimate of the MPC parameters. For each MPC, the estimated channel parameters are complex amplitude, delay, and DoA (ϕ, θ). The number of iterations in SAGE is set to 30 and 50 MPCs are estimated.

V. Measurement Setup

Channel measurements are performed using the RUSK Lund channel sounder. The channel sounder measures the complex transfer function of the radio channel between the Tx and Rx antennas at different frequency points. In the measurements, three panel antennas are used as three different access point antennas, transmitting a channel sounding signal with center frequency at $2.44\,\text{GHz}$ and a bandwidth of $80\,\text{MHz}$. The channel sounder is based on a switched array architecture and it selects one of the Tx antenna at one time to transmit the sounding signal. The panel antennas have a gain of $10\,\text{dBi}$ in the main direction and having a beam width of $60°$ in the horizontal plane and $45°$ in the vertical plane.

To synchronize the recordings of the IMU and channel sounder, a TTL trigger signal is used to trigger the measurements at the channel sounder and the IMU measurements. A LabVIEW application is used to generate the trigger signal using the NI-9401 Digital Input/output module.

At the receiver side, a monopole antenna that has uniform antenna gain in the azimuth plane, is used to receive the incoming radio signal. The receiver antenna is also attached with a low cost inertial measurement unit, Phidget-1044. The IMU sampling rate was set to $250\,\text{Hz}$ for the data recording. The IMU has a 3-axis accelerometer, gyroscope, and magnetometer installed on it. For our measurements, only acceleration and gyro measurements are used to estimate the local coordinates of the array. The IMU can provide acceleration values upto $\pm 2g$ and rotation speed upto $\pm 300°/s$ for z-axis and $\pm 400°/s$ for x-, and y-axis measurements.

Since low cost IMUs are prone to static bias and offset errors static bias errors in the acceleration measurements are calibrated out using the Newton's method [6], alongwith cross-axis misalignment errors before applying the dead reckoning solution.

The measurements are performed in an indoor environment at one of the lecture theater halls in the E-building of LTH, Lund University, Sweden. The layout of the room in terms of antenna positions is shown in Fig. 5. This is a rich scattering environment as many different objects can contribute to different reflection paths for the radio wave from the transmitter to the receiver. To show some details about the setup, a photo is given in Fig. 6. Our main interest in this measurement campaign was to identify the line-of-sight (LOS) path from the incoming radio signal at the receiver.

Multiple free movements are carried out where the Rx antenna is moved freely in an arbitrary path. The true movement path is not tracked for these measurements, but the only validation for the suggested method is the DoA estimation results for the different LOS paths from different Tx antennas.
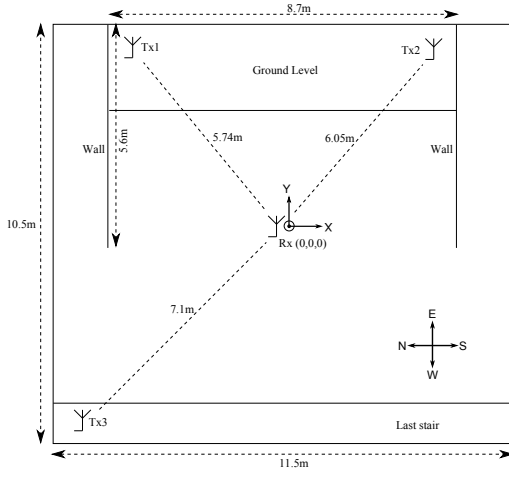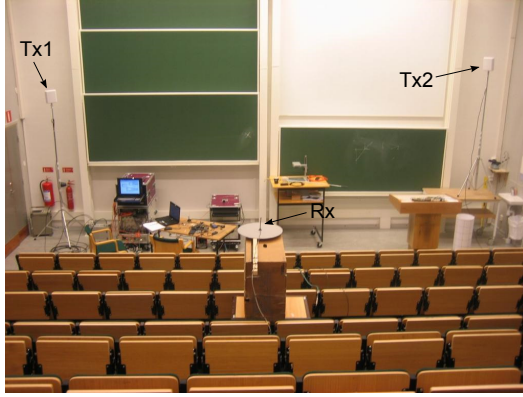
Fig. 5.   Room layout with antenna locations.

Fig. 6.   An indoor, rich scattering environment.

VI. RESULTS

The array coordinates are estimated from the IMU measurements of acceleration and angular speed. Fig. 7 shows the estimated location of the Rx antenna at different time instants during the movement. Here we have selected one of the measurement (Mov #2) from our data set of 43 different measurements that we have recorded during the measurement activity.

As the integration error in position estimates grows unboundedly over integration time [5], initial four seconds of the movement data is used for position estimation. Furthermore, to reduce the computation time of the SAGE algorithm, every 4th data sample is used from the estimated position values. The mean distance between two consecutive array positions is about $\lambda/10$ while maximum distance is observed to be around $\lambda/4$, where λ is the wavelength.

Using the estimated values of the array coordinates, DoA estimation is performed using 250 Rx antenna locations to form the virtual antenna array. As we have three independent radio links between the transmitter and receiver antennas, the SAGE estimates for these three links are determined independently.

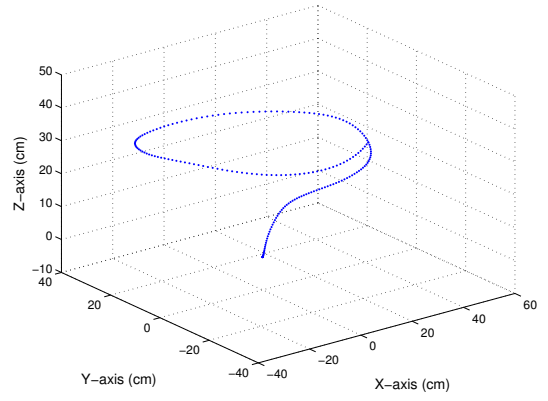Table I shows a comparison of the estimated values for

Fig. 7.   Array coordinates estimates using dead reckoning.

DoA. The estimated DoA for the LOS path is determined by comparing the estimated delay values of the significant MPCs with each other. The significant MPCs are selected based on the criterion that it can have upto $6\,$dB lower power as compared to the strongest MPC. The significant MPC which has the smallest estimated delay is selected as the LOS path. Fig. 8 shows the estimated DoA for different movements. Solid lines represent the true values for the DoA, while different markers on the dashed lines represent the estimated values for the DoA from different movements. Also, standard deviation values are computed for the DoA estimates in different measurements. A standard deviation of about $20°$ is observed for the estimates. But, for Tx2, a high value of standard deviation in azimuth could be the result of 2-3 outliers in the data as shown in Fig. 8.

TABLE I
SAGE ESTIMATES FOR DoA(ϕ, θ)

Tx Ant #	True Angle (ϕ, θ)	Estimated Angle Mov #2 (ϕ, θ)	Estimated Angle St. Deviation (ϕ, θ)
1	$(127°, 90°)$	$(120°, 89°)$	$(14°, 21°)$
2	$(47°, 80°)$	$(44°, 78°)$	$(33°, 21°)$
3	$(223°, 71°)$	$(220°, 71°)$	$(20°, 23°)$

The estimated DoA results for Mov #2 are shown in Figs. 9 - 11, where a polar plot is used to represent the estimated angles in the azimuth plane together with their respective estimated powers. Different points in the plot represent different MPCs. The dynamic range for this plot is set to $15\,$dB which will discard all those MPCs whose power is $15\,$dB lower than the power of the strongest MPC. The distance from the center of the circle represents the associated power with each MPC. The power of the MPCs is scaled such that the strongest MPC has power of $15\,$dB, and is located on the outer circle in the plots.

Future work includes detailed investigation about the size and shape of the antenna array such that the DoA(ϕ, θ) estimation error could be minimized. Also, less complex estimation algorithms to identify the LOS path in an indoor scenario will be investigated. Furthermore, the application of this antenna array technique would be tested with commercial
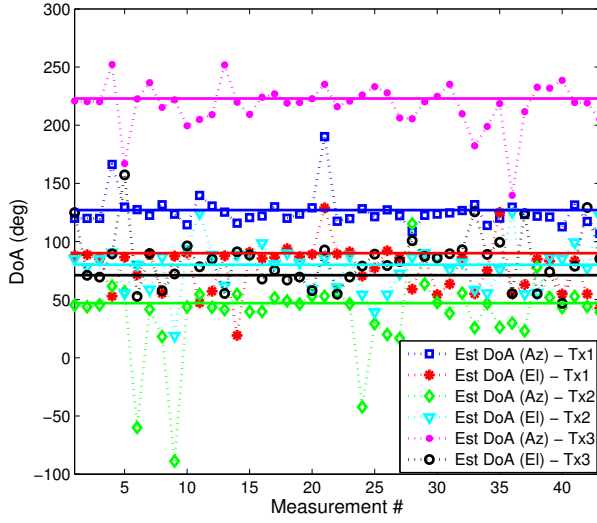
Fig. 8. DoA estimates of the LOS component using SAGE algorithm for multiple movements.
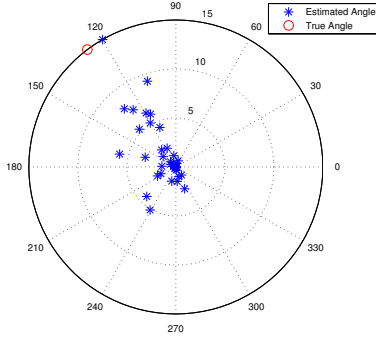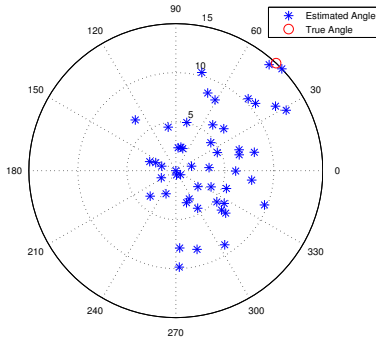
cellular networks, such as, the GSM network. For cellular networks, positioning/localization will be performed using DoA information of multiple base station antennas.

VII. CONCLUSION

In this paper, we have demonstrated a method to perform DoA estimation with single antenna devices using virtual arrays and random movements. It is shown that simple dead reckoning solution can be used for position estimation with low cost MEMS based inertial measurement units for short duration of the movement (for around 3-4 seconds). The position estimates are utilized for making virtual antenna arrays with single antenna devices for directional channel estimation. It has further been shown that the direction of arrival estimation by using a high resolution SAGE algorithm provides reasonably good accuracy with random virtual antenna arrays.

REFERENCES

[1] Andreas F. Molisch, *Wireless Communications*, ISBN 0-470-84887-1, Wiley, 2005.
[2] Yvo L.C. de Jong, Matti H. A. J. Herben, *High-Resolution Angle-of-Arrival Measurement of the Mobile Radio Channel*, IEEE Transactions on Antennas and Propagation, Vol. 47, No. 11, Nov. 1999.
[3] A. Broumandan, T. Lin, A. Moghaddam, D. Lu, J. Nielsen, G. Lachapelle, *Direction of Arrival Estimation of GNSS Signals Based on Synthetic Antenna Array*, ION GNSS 2007, Fort Worth, TX, Sept. 25-28, 2007.
[4] B. H. Fleury, M. Tschudin, R. Heddergott, D. Dahlhaus, and K. I. Pedersen, *Channel parameter estimation in mobile radio environments using the SAGE algorithm*, IEEE J. Select. Areas Commun., vol. 17, no. 3, pp. 434-450, Mar. 1999.
[5] Wall, J.H., Bevly, D.M., *Characterization of Inertial Sensor Measurements for Navigation Performance Analysis*, ION GNSS 2006, Fort Worth, TX, September 2006, pp. 2678-2685.
[6] Isaac Skog, Peter Händel, *Calibration of a MEMS Inertial Measurement Unit*, XVII IMEKO World Congress, Sept. 17-22, 2006.
[7] Phillips, W. F., Gebert, G. A., and Hailey, C. E., *Review of Attitude Representations Used for Aircraft Kinematics*, Journal of Aircraft, Vol. 38, No. 4, July-August 2001, pp. 718-737.

Fig. 9. DoA estimates for Mov #2 using SAGE algorithm: Tx1-Rx.

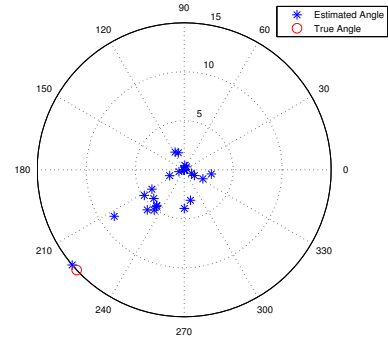Fig. 10. DoA estimates for Mov #2 using SAGE algorithm: Tx2-Rx.

Fig. 11. DoA estimates for Mov #2 using SAGE algorithm: Tx3-Rx.